Published in: Journal of Physics: B Atomic Molecular & Optical Physics (2014), vol. 47, 085101.
Status: Postprint (Author's version)

The threshold photoelectron spectrum of the geminal chloro-fluoro-ethene (1,1-C_2H_2FCl) isomer. Experiment and theory

R Locht[1], D Dehareng[2] and B Leyh[1]

[1] *Molecular Dynamics Laboratory, Department of Chemistry, Institute of Chemistry, University of Liège, Bldg B6c, Sart-Tilman, B-4000 Liège 1, Belgium*

[2] *Department of Life Sciences, Centre for Protein Engineering, Institute of Chemistry, University of Liège, BldgB6a, Sart-Tilman, B-4000 Liège 1, Belgium*

Abstract

The threshold photoelectron spectrum (TPES) of 1,1-C_2H_2FCl has been measured for the first time using synchrotron radiation. It has been compared to the HeI PES obtained earlier (Tornow *et al* 1990 *Chem. Phys.* **146** 115). Eight photoelectron bands have been observed at 10.22, 12.45, 13.28, 14.29, 14.99, 17.12, 17.67 and at 20.23 eV successively. Only the first three bands exhibit a rich and extensive vibrational structure. Their adiabatic ionization energies are measured and a detailed vibrational analysis is presented. The assignments of the electronic bands and of the vibrational wavenumbers were made by using *ab initio* quantum chemical calculations. These allowed us to provide the MO description of the eight electronic states in terms of ionization and double excitation. The good correlation between predicted vibrational wavenumbers and the experimental values provides a strong basis for the assignment of all the vibrational structures.

Keywords: synchrotron radiation, threshold photoelectron spectroscopy, quantum chemical calculations, vibrational structure, autoionization, electronic excitation, 1,1-C_2H_2FCl

Online supplementary data available from stacks.iop.org/JPhysB/47/085101/mmedia

1. Introduction

Recently, the high resolution vacuum UV photoabsorption spectrum (PAS) of the geminal 1,1-C_2H_2FCl has been measured and analysed in detail [1]. The Rydberg series and their vibrational structures have been investigated and assigned. *Ab initio* quantum chemical calculations were applied to the neutral and first excited states of the molecule. In an earlier paper devoted to the three C_2H_2FCl isomers, Tornow *et al* [2] described the respective HeI (21.22 eV/58.4 nm) and NeI (16.67-16.87 eV/74.37-73.58 nm) photoelectron spectra. The successive ionization energies were interpreted with the help of MNDO calculations. Assignments of the observed vibrational structures were proposed.

The aim of the present paper is to complete the work on the 1,1-C_2H_2FCl molecular system by reporting on the threshold photoelectron spectrum (TPES) in the 9.0-24.0 eV spectral region using synchrotron radiation. The new light shed by our recent vacuum UV PAS [1] and the use of quantum chemical calculations applied to the cationic system will support our analysis and assignments.

2. Experimental details

2.1. Experimental setup

The experimental setup used in this work has already been described in detail elsewhere [3]. Only the most salient features will be reported here.

Synchrotron radiation available from the BESSY II facility (Berlin, Germany) was dispersed with at 3m-NIM-2 beam line. The 3m-NIM monochromator is positioned at a bending magnet front end. It is equipped with two spherical gratings, i.e., an Al/MgF_2-grating of 600 l/mm and a Pt-grating of 2 4001/mm allowing us to scan the 5-55 eV photon energy range. The latter grating has its optimal transmission between 10 and 40 eV

(124-31 nm). The entrance and exit slits were adjusted between 100 and 200 µm. Owing to the second order contribution at low photon energy, a LiF window is used when necessary, restricting the observations to an upper photon energy range of 11.8 eV.

For the TPES experiments the light beam is focused into an ion chamber, in the focussing plane of a tandem electron spectrometer consisting of two 180° electrostatic deflectors. This electron energy analyser works at constant energy resolution, i.e., at constant pass energy E_0. The resolution defined as the full-width at half-maximum (FWHM) is given by $\Delta E/E_0 = w/104$ where w is the slit width expressed in millimetres. In the present experiments w = 0.5 or 1.0 mm and E_0 is set at 1.1 to 10.0 V depending on the type of experiment and on the signal intensity.

Figure 1. *TPES spectrum of Ar between 15.70 and 16.0 eV as measured in the experimental conditions used in the present work. The FWHM is 5 meV.*

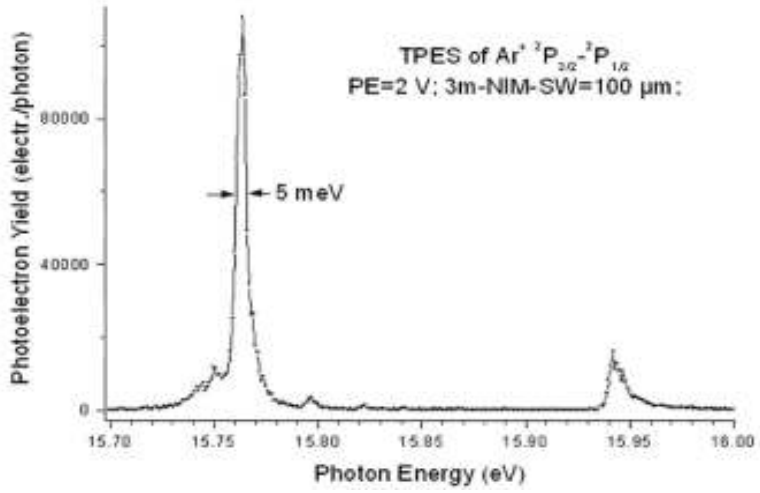

The TPES operating mode corresponds to 'constant photoelectron energy' spectroscopy. These spectra are recorded by tuning the photon energy hv and keeping constant the kinetic energy, E_{kin}, of the electrons transmitted through the tandem electron energy analysers system. Therefore, the electron accelerating voltage V_{acc} is kept as close as possible to E_0, transmitting only 'zero-kinetic energy' or 'threshold' (TPE) photoelectrons. In practice, a fine tuning of V_{acc} is performed to optimize the TPE signal intensity. Figure 1 shows the TPES of $Ar^+(^2P_{3/2}\text{-}^2P_{1/2})$ as measured in the optimal conditions used for the following experiments. A global 5 meV photoelectron energy resolution is achieved. Moreover, the same figure shows the discrimination power of the electron energy analyzer: the intensity ratio of the 30 meV and threshold photoelectrons is about 3%.

In addition to the synchrotron storage ring beam current, the photoelectron signal of a gold diode, inserted in the ion chamber at the opposite of the 3m-NIM monochromator exit slit, is measured in order to normalize the photoelectron signals to the monochromator transmission function.

Two different samples of 1,1-C_2H_2FCl have been used. A first sample was prepared in the laboratory as described earlier [2] and was of 99.9% gas chromatographic purity with a boiling point of -24 °C. The commercially available 1,1-C_2H_2FCl, purchased from ABCR GmbH and of 98% purity, was used without further purification. No difference has been observed between the spectra recorded with both samples.

2.2. Data handling and error estimation

As will be mentioned in the next sections, weak sharp peaks and diffuse structures are often superimposed on a strong continuum. To make the characterization of these features easier, a continuum subtraction procedure has been applied. This method has already been used successfully in previous spectral analyses [4, 5]. For this purpose, the experimental curve is severely smoothed to simulate the underlying continuum which is then subtracted from the original spectrum. The smoothing procedure consists in filtering the experimental curve by fast Fourier transform. The weak features emerge from a remaining strongly attenuated background. The resulting diagram will be called Δ-plot in the forthcoming sections. This procedure is free from spurious structure generation. To verify that no weak structure has been removed by this operation, the same procedure is applied to the subtracted continuum. The result is a signal oscillating about zero with amplitudes of about two orders of magnitude or even lower than the signal resulting from the first operation. On the other hand,

the reverse operation consisting in the summation of the smoothed curve and the 'Δ-plot' restores the original signal. This data handling procedure has been thoroughly investigated and validated by Carbonneau [6] and Marmet [7]. A more detailed description of this data processing is included as supplementary data (available at stacks.iop.org/JPhysB/47/085101/mmedia) to this paper.

The wavelength calibration of the 3m-NIM monochromator has been performed by using the Ar absorption spectrum between the $^2P_{3/2}$ and the $^2P_{1/2}$ ionic states. The repeated recording of this spectrum shows the accuracy of this calibration to be 2-3 meV. In the measurements between 9 and 24 eV photon energy, the TPES spectrum has been recorded with energy intervals of about 10 meV. The error on the energy position of a feature is estimated to be 6 meV. In the TPES spectra recorded between 10 and 14 eV an energy increment of 2 meV has been adopted. The error on the energy position of a feature is estimated to be of the order of 3 meV. This estimation is confirmed by the reproducibility of energy positions measured in different spectra recorded over several measurement sessions.

Figure 2. *(a) TPES spectrum of 1,1-C_2H_2FCl between 9.5 and 23.0 eV photon energy compared to the HeI-PES as normalized to the vertical ionization transition in the $\tilde{X}^2A''$ state. (b) The 9.9-13.9 eV TPES spectrum under higher resolution. For both spectra the most important experimental conditions are indicated. Vertical bars indicate the critical energies.*

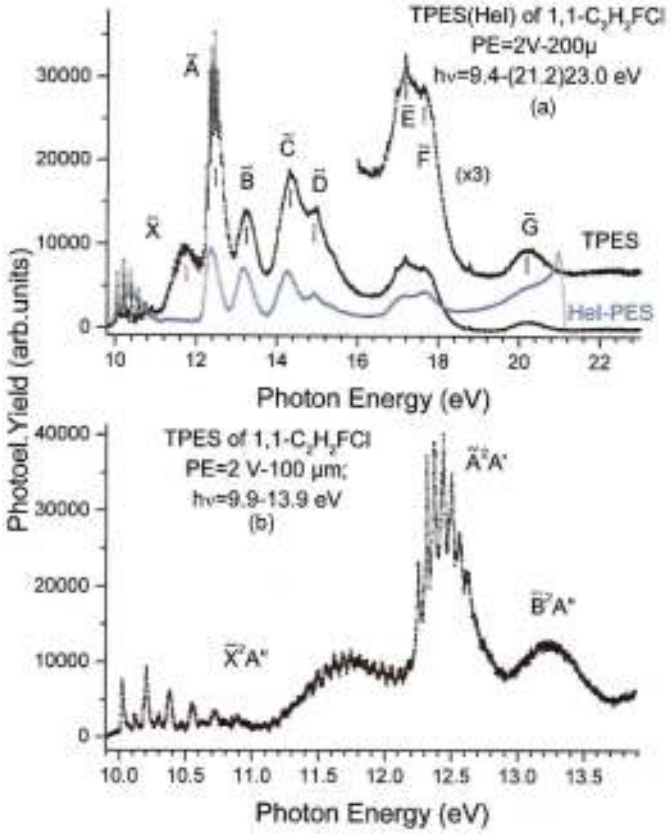

3. Experimental results

Figure 2(a) shows the TPE spectrum of 1,1-C_2H_2FCl recorded over a wide photon energy range, i.e., from 10 to 23 eV, and with 10 meV energy increments. The upper limit was restricted by the grating transmission function.

Eight well-defined bands are observed and their vertical ionization energies are listed in table 1. A new strong, broad and strongly structured band peaks at about 11.7 eV.

For comparison, the HeI-PES is reproduced in the same figure, normalized to the intensity of the vertical transition in the first PES band. The vertical ionization energies determined in this spectrum are also

listed in table 1 together with the NeI-PES results [2]. The TPES measured with increments of 2 meV between 9.9 and 13.9 eV is displayed in figure 2(b).

***Table 1**. Adiabatic and vertical ionization energies (eV) measured by HeI-PES, NeI-PES [2] and by TPES using synchrotron radiation.*

Tornow *et al* [2]				This work	
HeI[a]		NeI[a]		TPES[b]	
IE_{ad}	IE_{vert}	IE_{ad}	IE_{vert}	IE_{ad}[c]	IE_{vert}
10.02	10.17	10.02	10.21	10.035	10.22
12.24	12.40	12.22	12.35	12.245	12.44
12.97	13.22	13.00	13.24	-	13.28
13.95	14.25	-	14.27	-	14.29
-	14.93	-	14.94	-	14.99
-	17.17	-	-	-	17.12
-	17.69	-	-	-	17.67
-		-	-	-	20.23

[a] Uncertainty ± 0.02 eV [2].
[b] Uncertainty ± 0.006 eV, see section 2.2.
[c] Uncertainty ± 0.003 eV, see section 2.2.

As observed in many cases, large differences between the HeI-PES and the TPES appear in figure 2(a). Compared to the intensity of the $\tilde{X}^2A''$-band of the ionic ground state at 10.199 eV, the relative intensity of the PES-bands corresponding to the ionic excited states is considerably enhanced by resonant photoionization in the TPES. The very long vibrational progression in the $\tilde{X}^2A''$ ground ionic state of 1,1-C_2H_2FCl shows up very clearly with a maximum intensity at about 11.7 eV. As already observed in the case of 1,1-$C_2H_2F_2$ [8], the intensity in the HeI-PES is shared between the ground and the excited states of the ion, whereas the TPES is overwhelmingly dominated by the excited states between 12 and 21eV.

4. *Ab initio* calculations: methods and results

4.1. Computational tools

All the calculations were performed with the Gaussian 09 program [9]. The basis set used for all the calculations is aug-cc-pVDZ [10] containing polarization as well as diffuse functions. The geometry optimization has been performed at the CCSD(FC) [11, 12] and M06-2X(DFT) [13] levels.

The molecular orbital configuration of 1,1-C_2H_2FCl in the C_S symmetry group is described by

$$\begin{aligned} &1s(Cl)^2,\ 2s(Cl)^2,\ 1s(F)^2,\ 1s(C1)^2,\ 1s(C2)^2,\ 2p_{x,y,z}(Cl)^6 \\ &(1a')^2\ (2a')^2\ (3a')^2\ (4a')^2\ (5a')^2\ (1a'')^2\ (6a')^2\ (7a')^2 \\ &\times(8a')^2\ (2a'')^2\ (9a')^2\ (3a'')^2 : \tilde{X}^1A' \end{aligned}$$

where 1a' and 2a' are the first outer-valence shell orbitals. Adiabatic ionization energies of eight cationic states have been calculated at the CASSCF [14-16] level with the state average option, and with two different active spaces, CAS(5,8) (2a", 9a', 3a"//10a', 11a', 12a', 4a", 13a') and CAS(9,8) (1a', 8a', 2a", 9a', 3a"//10a', 4a", 11a'). The geometry optimization of the $\tilde{B}$ excited state was performed at the TDDFT level [17] with the M06-2X functional. As is usual for wavenumber values, a scaling factor was applied and chosen to be the same as for B3LYP/6-31+G** (0.96) as given by Irikura *et al* [18].

4.2. Results of the calculations

The result of the geometry optimization of the neutral $\tilde{X}^1A'$ ground state and of the cationic ground $\tilde{X}^2A''$ and first two excited states $\tilde{A}^2A'$ and $\tilde{B}^2A''$ are presented in table S1 (see the supplementary data (available at stacks.iop.org/JPhysB/47/085101/mmedia)), according to the atomic numbering shown in the same table, and at two different calculation levels. In the literature, the calculation level which is considered as the most accurate is CCSD(FC), but the M06-2X is also recognized as a very good functional [11]. The two methods belong to different calculation frameworks, a wavefunction-based or a density functional-based approach, respectively. Since the electronic correlation is not parametrized in the first case, it provides results that are supposed to be

less dependent on the nature of the molecular systems considered.

The vibrational normal modes of the cationic ground state $\tilde{X}^2A''$ and the first two excited states $\tilde{A}^2A'$ and $\tilde{B}^2A''$ of the molecular ion are represented in figures S1-S3 (available at stacks.iop.org/JPhysB /47/085101/mmedia). For the latter two states only those normal modes differing from the ionic ground state are shown. The corresponding wavenumbers predicted by the present calculations are listed in table S2 (see the supplementary data (available at stacks.iop.org/JPhysB/47/085101/mmedia)). Furthermore, the important elongation of the C-Cl internuclear distance has to be pointed out, i.e. 0.35 Å between the neutral $\tilde{X}^1A'$ ground state and the $\tilde{B}^2A''$ cationic state. Therefore, the C-Cl bond has been represented by a dashed line in figure S3 (see the supplementary data (available at stacks.iop.org/JPhysB/47/085101/mmedia)).

The vertical ionization energies of 1,1-C_2H_2FCl as calculated at two CASSCF levels are listed in table 2, together with their corresponding MO description. Several ionization energies are described by doubly excited (ionization/excitation) configurations.

Table 2. *Vertical ionization energies (eV) calculated at the CAS(5,8)/aug-cc-pVDZ and at CAS(9,8)/aug-cc-pVDZ levels with respect to the neutral ground state $\tilde{X}^1A'$ (ionic $\tilde{X}^2A''$ ground state). MO descriptions include simple ionization (SI) as well as ionization and excitation (IE) configurations.*

Level	IE_{vert}(eV)	MO description
CAS(5,8)/aug-cc-pVDZ	9.89 (0.0)	$(2a'')^2\ (9a')^2\ (3a'')^1$ (SI)
	11.79 (1.90)	$(2a'')^2\ (9a')^1\ (3a'')^2$ (SI)
	12.89 (3.00)	$(2a'')^1\ (9a')^2\ (3a'')^2$ (SI)
	16.11 (6.22)	$(2a'')^2\ (9a')^2\ (4a'')^1$ (IE)
	16.24 (6.35)	$(2a'')^2\ (9a')^1\ (3a'')^1\ (4a'')^1$ (IE)
	16.96 (7.07)	$(2a'')^2\ (9a')^2\ (13a')^1$ (IE)
	17.26 (7.37)	$(2a'')^2\ (9a')^1\ (3a'')^1\ (10a')^1$ (IE)
	18.27 (8.38)	$(2a'')^2\ (9a')^1\ (3a'')^1\ (10a')^1$ (IE)
CAS(9,8)/aug-cc-pVDZ	9.53 (0.0)	$(7a')^2\ (8a')^2\ (2a'')^2\ (9a')^2\ (3a'')^1$ (SI)
	11.74 (2.21)	$(7a')^2\ (8a')^2\ (2a'')^2\ (9a')^1\ (3a'')^2$ (SI)
	12.54 (3.01)	$(7a')^2\ (8a')^2\ (2a'')^1\ (9a')^2\ (3a'')^2$ (SI)
	14.61 (5.08)	$(7a')^2\ (8a')^1\ (2a'')^2\ (9a')^2\ (3a'')^2$ (SI)
	15.65 (6.12)	$(7a')^1\ (8a')^2\ (2a'')^2\ (9a')^2\ (3a'')^2$ (SI)
	15.93 (6.40)	$(7a')^2\ (8a')^2\ (2a'')^2\ (9a')^2\ (4a'')^1$ (IE)
	16.29 (6.76)	$(7a')^2\ (8a')^2\ (2a'')^2\ (9a')^1\ (3a'')^1\ (4a'')^1$ (IE)
	17.23 (7.70)	$(7a')^2\ (8a')^2\ (2a'')^2\ (9a'')^2\ (11a')^1$ (IE)

5. Discussion

5.1. The TPE spectrum of 1,1-C_2H_2FCl between 9.5 and 23.0 eV (see figure 2)

The two CAS calculations described in the previous section agree to interpret and assign the first three PES bands observed in figure 2(a) to the ionization of the 3a", 9a' and 2a" MO successively. The corresponding states are then $\tilde{X}^2A''$, $\tilde{A}^2A'$ and $\tilde{B}^2A''$ respectively. The CAS(9,8) level which takes into account the 7a' and 8a' MOs is able to account for the vertical energies observed at 14.2-14.3 eV and at 14.93-14.99 eV (see table 1), which can then be assigned to single ionization from these 7a' and 8a' orbitals leading to the $\tilde{C}^2A'$ and the $\tilde{D}^2A'$ cationic states.

Both calculation levels agree in assigning the higher energetic bands to doubly excited configurations, i.e. ionization together with excitation to a virtual MO. Two of these are close in energy, differing by 0.30 or 0.36 eV by CAS(5,8) and CAS(9,8) respectively. They correspond to ^{2}A' and ^{2,4}A" or ^{2}A" and ^{2,4}A' states, respectively. The transitions to this pair of satellite states, which can only borrow intensity from interactions with singly-excited configurations and which are therefore expected to be weak, happen to lie in the same energy region as that of the $\tilde{E}$ and the $\tilde{F}$ (single ionization) bands observed at 17.12-17.17 eV and at 17.67-17.69 eV (see table 1).

The weak TPES band observed at 20.23 eV is very likely to be described by the $(9a')^1\ (3a'')^1\ (10a')^{12,4}$A' (at the CAS(5,8) level) or by the $(2a'')^2\ (9a'')^2\ (11a')^{12}$A' (at the CAS(9,8) level) doubly excited configurations.

This would also be the reason for the weakness of the transition.

Remarkably, only the two first ionic states, i.e. $\tilde{X}^2A''$ and $\tilde{A}^2A'$ bands exhibit a very well defined vibrational structure. Even at high resolution conditions, and starting with the $\tilde{B}^2A''$ state, the TPES bands correspond to continua.

Tornow [19] and Kaufel [20] investigated the ionization and dissociation of 1,1-C2H_2FCl by photoionization mass spectrometry using synchrotron radiation between 9 and 20 eV and dissociative electroionization [21]. Their results indicate that about 96% of the ionization and dissociation occurs between 10.04 and 17.55 eV. The lowest appearance energy (AE) is measured at 12.91 eV [20] for the $C_2H_2F^+$ fragment representing 50% of the total ionization at a photon energy of 20 eV whereas the intensity of the molecular ion is 18% at the same energy. This AE corresponds very well to the IE_{ad} estimated at 12.97 eV for the $\tilde{B}^2A''$ state (see table 1). A TPIPECO experiment would provide support to this correlation and a deeper insight to the dynamics of this cationic state. In the 13.75-14.99 eV region corresponding to the $\tilde{C}^2A'$-$\tilde{D}^2A'$ ionic states, all other halogenated fragment ions are generated.

Figure 3. *Vibrational analysis of (a) the TPES spectrum of the $\tilde{X}^2A''$ band of 1,1-C_2H_2FCl and (b) its corresponding Δ-plot. Vertical bars indicate critical energies and vibrational structure.*

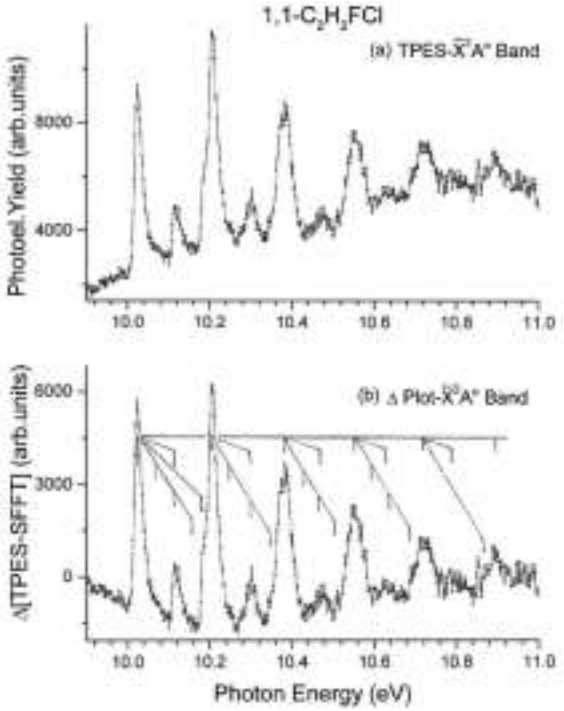

5.2. The $\tilde{X}^2A''$ TPES band (see figures S1 and 3)

The TPES of the $\tilde{X}^2A''$ band of 1,1-C_2H_2FCl is shown in figure 3(a) between threshold and 11.0 eV photon energy. The shape of the $\tilde{X}^2A''$ band in the TPES of 1,1-C_2H_2FCl is closely similar to that of the $\tilde{X}^2B_1$ band observed in the TPES of 1,1-$C_2H_2F_2$ [6]. Weak signals are observed at about half the interval between the major peaks. In 1,1-C_2H_2FCl they are stronger than in 1,1-$C_2H_2F_2$.

To enhance the small structures in this first band, the subtraction method has been applied to it (see section 2.2 and the supplementary data (available at stacks.iop.org/JPhysB/47/085101/mmedia): the result is shown in figure 3(b). The energy positions of the successive structures are listed in table 3. The uncertainty mentioned for each position represents the largest deviation from the average of five independent measurements. Obviously the main vibrational structure starts at 10.034 ± 0.005 eV and corresponds to the adiabatic ionization energy IE_{ad}. This IE has to be compared to the value determined by HeI- and NeI-PES, i.e. at 10.024 ± 0.010 eV [2]. An IE_{ad} = 10.04 eV has been measured by mass spectrometric photoionization using synchrotron radiation [19, 20]. The energy of 10.199 ± 0.003 eV corresponds to the vertical ionization energy and can be compared to

10.17 and 10.21 eV as measured by HeI-PES and NeI-PES, respectively [2].

Table 3. *Energy positions (eV) of the structures observed in the $\tilde{X}^2A''$ HeI-PES and TPES of 1,1-C_2H_2FCl. Assignments and experimental wavenumbers (eV/cm^{-1}) are listed. Conversion factor 1 eV = 8 065.545 cm^{-1} [22].*

$\tilde{X}^2A''$ Band structure			
HeI[a] [2]	TPES[b]	Assignments	Average wavenbr/energy
10.025	10.034 ± 0.005	0,0	ω_3 = 1476 ± 16 cm^{-1}
10.082	10.079 ± 0.007	ν_9	or 183 ± 2meV
10.122	10.124 ± 0.004	$\nu_7/2\nu_9$	ω_3x_3 = 16 ± 4 cm^{-1}
10.163	10.164 ± 0.004	$3\nu_9$	or 1.9 ± 0.6 meV
10.185	10.199 ± 0.003	na	
10.202	10.216 ± 0.004	$\boldsymbol{\nu_3}$	ω_7 = 750 ± 56 cm^{-1}
10.256	10.255 ± 0.006	$\nu_3+\nu_9$	or 93 ± 7 meV
10.299	10.286 ± 0.002	na	
10.342	10.311 ± 0.006	$\nu_3+\nu_7$	ω_9 = 347 ± 40 cm^{-1}
10.342	10.361 ± 0.005	$\nu_3+3\nu_9$	or 43 ± 5 meV
10.374	10.390 ± 0.009	$\boldsymbol{2\nu_3}$	
10.430	10.444 ± 0.010	$2\nu_3+\nu_9$	
10.493	10.482 ± 0.009	$2\nu_3+\nu_7$	
10.529	10.529 ± 0.007	$2\nu_3+3\nu_9$	
10.556	10.563 ± 0.007	$\boldsymbol{3\nu_3}$	
10.643	10.630 ± 0.017	na	
10.679	10.667 ± 0.012	$3\nu_3+\nu_7$	
10.718	10.705 ± 0.001	$3\nu_3+3\nu_9$	
10.751	10.733 ± 0.007	$\boldsymbol{4\nu_3}$	
10.811	10.819 ± 0.001	$4\nu_3+\nu_7$	
10.883	10.877 ± 0.006	$4\nu_3+3\nu_9$	
	10.900 ± 0.007	$\boldsymbol{5\nu_3}$	

[a] Estimated uncertainty: ± 0.010 eV
[b] Largest deviation from the average of five independent measurements.

The main features observed in the present band are clearly separated by a decreasing interval ΔG_v. This interval has been plotted versus the vibrational quantum number v as shown in figure 4. Including the total uncertainties on the intervals, a linear fit with a correlation coefficient of 0.96 provides two constants characterizing the $\tilde{X}^2A''$ ground state of 1,1-$C_2H_2FCl^+$: the vibrational energy $hc\omega_0$ = 183 ± 2 meV (1476 ± 16 cm^{-1}) and the anharmonicity coefficient $hc\omega_0x_0$ = 1.9 ± 0.6 meV (16 ± 4 cm^{-1}). This extrapolated wavenumber has to be compared to the averaged value 1400 ± 36 cm^{-1} measured by HeI-PES [2]. It has also to be compared to the scaled wavenumbers predicted by *ab initio* calculations. The data from table S2 (available at stacks.iop.org/JPhysB/47/085101/mmedia) show that two vibrational modes could be considered, i.e., ω_3 = 1479 cm^{-1} and ω_4 = 1372 cm^{-1}. The experimental wavenumber is very close to the scaled value of ν_3 corresponding to the *C*=C stretching motion with H-C-H bending (figure S1 (available at stacks.iop.org /JPhysB /47/085101/mmedia)). The first ionization energy corresponds to the removal of an electron from the 3a" MO which has a dominant π character. Furthermore, in all ethylene derivatives investigated previously [6, 23], the major vibrational motion in the first PES band is the *C*=C stretching vibration. Therefore, the most probable assignment of the 1476 cm^{-1} wavenumber is the ν_3 vibrational normal mode.

The weaker signal observed at about half the interval between the major progression is regularly observed at an average value of 93 ± 7 meV (750 ± 56 cm^{-1}) (see table 3). This spacing can correspond to 722 ± 14 cm^{-1} reported earlier [2]. This value corresponds very likely to ω_7 = 746 cm^{-1} predicted by the present calculations. This wavenumber is thus assigned to ν_7 described by the CH_2 rocking accompanied by C-F and C-Cl stretching motions (see figure S1 (available at stacks.iop.org/JPhysB/47/085101/mmedia)).

Very weak signals are measured in this band at very reproducible intervals of 43 ± 5 meV (347 ± 40 cm^{-1}) (see table 3). By HeI-PES a wavenumber of 380 ± 22 cm^{-1} has been measured [2]. The intensities in the TPES could indicate that we are dealing with a short progression of three quanta. Only v = 1 and 3 are observed, but v = *2* should be buried in the ν_7 peak, possibly giving rise to a Fermi resonance. Also in this case, the experimental value could be compared to the wavenumber calculated at 350 cm^{-1} and corresponding to ν_9, i.e. a complex vibrational motion affecting all angles and also the CH and CF bond lengths (figure S1 (available at stacks.iop.org/JPhysB/47/085101/mmedia)).

Finally, on the low-energy side of the second major peak a shoulder is observed lying at 10.199 eV. The corresponding energy interval is of 0.165 eV (1 331 cm^{-1}). This energy could correspond to the excitation of one quantum of the v_4 vibration predicted at 1 372 cm^{-1}. It corresponds to the CH_2 bending combined with the CF stretching. Owing to the strong anharmonicity on v_3 this structure would likely be hidden in the signal generated by the higher vibrational quanta of v_3.

Figure 4. *ΔG_v-versus υ plot for the first five v_3 vibrational levels of the $\tilde{X}^2A''$ band (black solid circles: experimental data points, red squares: calculated least-squares fit).*

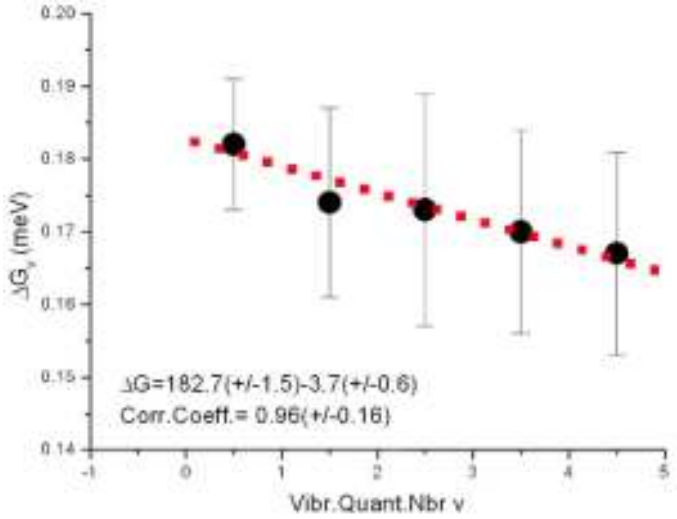

Figure 5. *Analysis of the Δ-plots of the (a) TPES and (b) PAS of 1,1-C_2H_2FCl in the photon energy region of 1,1-C_2H_2FCl between 11.2 and 12.2 eV. Vertical bars in the latter spectrum indicate the energy position of Rydberg states and their vibrational structure [1].*

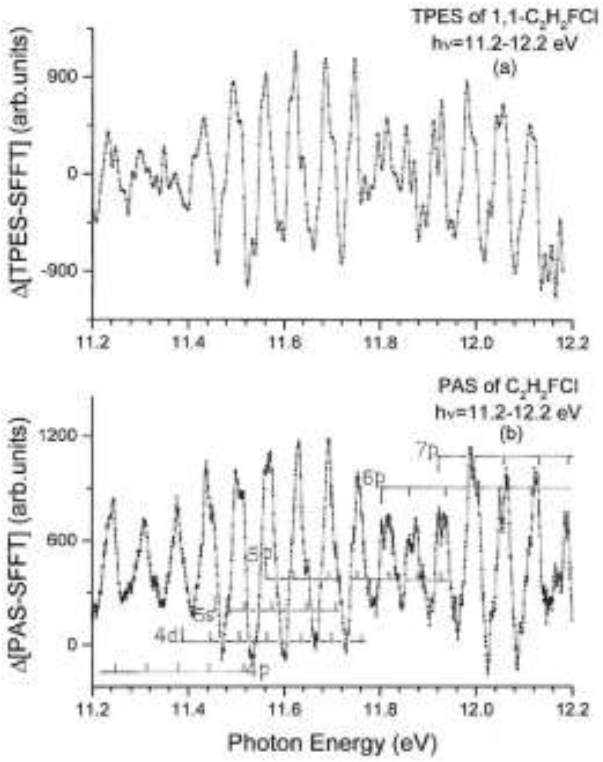

5.3. The $\tilde{X}$-$\tilde{A}$ intermediate photon energy region (see figure 5)

In the photon energy range of 11-12 eV no photoelectron current is detected in the HeI-PES (see figure 2(a)). Contrarily, in the TPES a strong photoelectron signal has been measured. Its intensity is even higher than

that of the $\tilde{X}^2A''$ band and has a rather complex structured band shape. For more clarity, the Δ-plot of the TPES has been reproduced in figure 5(a) between 11.2 and 12.2 eV.

Table 4. *Energy position (eV) of the features observed in the TPES between the $\tilde{X}^2A''$ and $\tilde{A}^2A'$ states of 1,1-$C_2H_2FCl^+$ and in the corresponding photon energy range of the vacuum UV PAS of 1,1-C_2H_2FCl [1].*

$\tilde{X}$-$\tilde{A}$ photon energy region	
PAS [1][a]	TPES (This work)[b]
11.244	11.243 ± 0.004
-	11.272 ± 0.010
11.307	11.312 ± 0.009
11.377	11.381 ± 0.008
11.438	11.440 ± 0.007
11.500	11.504 ± 0.010
11.563/11.567	11.569 ± 0.007
11.631	11.628 ± 0.006
11.650	11.653 ± 0.003
11.691	11.692 ± 0.010
11.709	11.708 ± 0.008
11.754/11.755	11.750 ± 0.009
11.804	11.808 ± 0.007
11.862	11.865 ± 0.004
11.923	11.921 ± 0.006
-	11.940 ± 0.005
12.049/12.064	12.053 ± 0.012
11.120/11.125	12.124 ± 0.006
-	12.158 ± 0.010
11.185	12.183 ± 0.009
-	12.214 ± 0.005

[a] Uncertainty ±0.003 eV [1].
[b] Largest deviation from the average of five independent measurements.

For comparison the Δ-plot of the vacuum UV PAS has been displayed in figure 5(b) as measured and discussed in detail in [1]. The high degree of correlation between the two types of spectra is very convincing as also shown in table 4.

The interpretation and assignments of the structure in the PAS [1] are included in figure 4(b). This part of the PAS was assigned to the electronic and vibrational excitation of np (n = 4-7), 4d and 5s Rydberg series, all converging to the $\tilde{A}^2A'$ cationic state.

The good correlation between both spectra is an indication about the fate of the identified Rydberg states. To provide 'zero kinetic energy' photoelectrons they all have to autoionize resonantly. The Rydberg states identified in the present investigation decay preferentially by resonant autoionization. Furthermore, most of the features listed in table 4 show energy intervals of about 62 ± 5 meV (500 ± 40 cm^{-1}). A likely interpretation would be the population of the upper part of the ionic ground state potential through electronic autoionization. Considering the intensity of the features observed between 11 and 12 eV, it is reasonable to consider that the continuation of the ν_3 vibrational progression is concerned in this photon energy range. Using the wavenumber and anharmonicity obtained for the first five vibrational levels of the $\tilde{X}^2A''$ ground state of the cation, the vibrational quanta in the neighbourhood of $\upsilon \approx 30$ would be involved. However, at that level higher order anharmonicity terms have to be introduced in the expression of the vibrational energy and the $\upsilon = 30$ level would be an upper or lower limit depending upon the sign and magnitude of the additional anharmonicity constants [24].

5.4. The $\tilde{A}^2A'$ and the $\tilde{B}^2A''$ TPES bands (see figures 2, S2 and 6)

The photon energy region of 12.0-13.8 eV is shown in figure 6(a) on an expanded energy scale. It clearly shows a broad and fairly strong band extending from 12.15 to 12.9 eV, exhibiting sharp structures. From 12.9-13.7 eV a weaker and structureless band has a maximum at about 13.28 eV.

To enhance the structure observed between 12.0 and 13.0 eV the subtraction method has been applied (see section 2.2 and supplementary data (available at stacks.iop.org/JPhysB/47/085101/mmedia). The resulting Δ-plot is displayed in figure 6(b) and clearly shows a complex vibrational structure. The position in energy of these features is listed in table 5 together with the earlier HeI- and NeI-PES measurements reported by Tornow *et al* [2].

Figure 6. *(a) TPES spectrum of 1,1-C_2H_2FCl in the 12-13.8 eV energy range and (b) the vibrational analysis of the Δ-plot of the $\tilde{A}^2A'$ band. Vertical bars indicate critical energies and vibrational structure.*

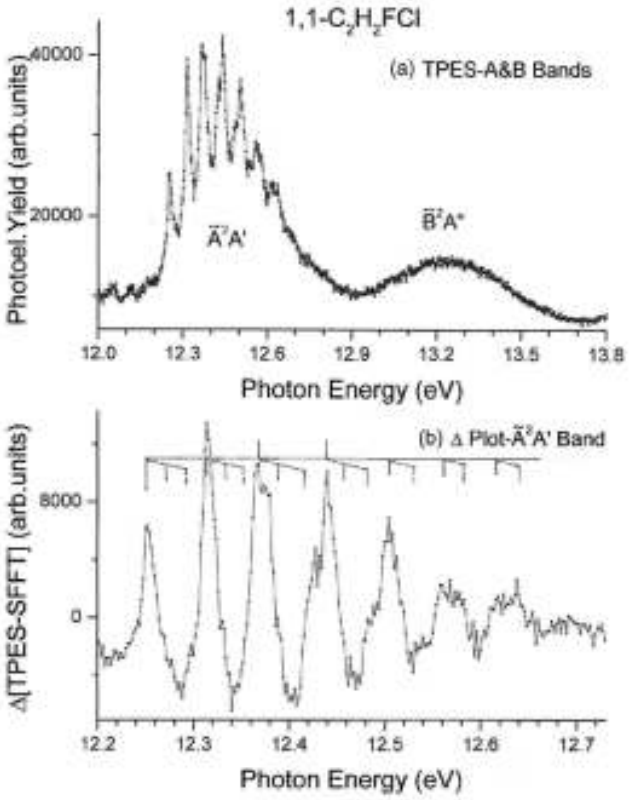

Between 12.0 and 12.2 eV, very weak residual structures are observed pertaining to the $\tilde{X}$ band as populated by autoionization (see previous section 5.3). The $IE_{ad}(\tilde{A}^2A')$ = 12.243 ± 0.009 eV is in very good agreement, within the error limits, with the values reported previously [2]. The $IE_{vert}(\tilde{A}^2A')$ = 12.303 ± 0.009 eV, corresponds to the second and most intense vibrational transition. This value agrees also with the previous measurements [2]. This observation indicates that the Franck-Condon distribution is not noticeably perturbed by the autoionization phenomenon.

Over the whole $\tilde{A}^2A'$ TPES band the strongest features are regularly spaced by 61 ± 4 meV or 492 ± 30 cm^{-1}. Compared to the results of the *ab initio* calculations presented in this work, this wavenumber has to be assigned unambiguously to the ν_7 vibrational mode predicted at 472 cm^{-1}. This vibration involves the in-plane CH_2 rocking superimposed to C-F and C-Cl stretching motions (see figure S2 (available at stacks.iop.org/JPhysB/47/085101/mmedia)). In the HeI- and NeI-PES a wavenumber of 524 ± 30 cm^{-1} was reported and assigned to the C-Cl stretching [2]. Six vibrational quanta of this mode are observed and no anharmonicity could be detected.

A further analysis of the $\tilde{A}^2A'$ TPES band reveals weak but fairly regular structures at intervals of 26 ± 4 meV or 210 ± 32 cm^{-1} as averaged over all measured values. This value is significantly lower than the wavenumber reported earlier by Tornow *et al* [2], i.e. 291 ± 30 cm^{-1}. By quantum chemical calculations a wavenumber of 220 cm^{-1} is predicted for the ν_9 bending motion affecting all intramolecular angles (see figure S2 (available at stacks.iop.org/JPhysB/47/085101/mmedia). This assignment is unambiguous.

The third $\tilde{B}^2A''$ ionic state extends between 12.9 and 13.7 eV. Its maximum is measured at about 13.28 eV, in agreement with the HeI- (13.22 eV) and NeI-PES (13.24 eV) results [2]. Figure 6(a) seems to indicate that

no vibrational structure is observed in this band, at least within a reasonable signal/noise ratio. From the present quantum chemical calculations a strong C-Cl elongation of 0.34 Å is highlighted in the $\tilde{B}^2A''$ state (see table S1 and figure S3 (available fromstacks.iop.org/JPhysB/47/085101/mmedia)). It should be plausible that among the excited vibrational modes one should find the ν_8 and ν_9 modes related to the geometry changes from the neutral to the cation $\tilde{B}^2A''$ state (see figure S3 (available from stacks.iop.org/JPhysB/47/085101/mmedia)). As already mentioned earlier (see section 5.1) dissociative photoionization experiments measured the threshold for the appearance of the most abundant fragment ion $C_2H_2F^+$ at 12.91 eV [20]. There is often a close correlation between the threshold energy of a continuum and the onset energy of (a) fragmentation(s). To answer this question TPEPICO and PEPICO experimental data are needed but not available today. Obviously TPEPICO or PEPICO, together with *ab initio* calculations will allow us to have a deeper insight on the dynamics of the process.

Table 5. *Energy positions (eV) and assignments of the structures observed in the HeI-, NeI-PES and TPES of the* $\tilde{A}^2A'$ *band of the 1,1-*$C_2H_2FCl^+$ *cation.*

$\tilde{A}^2A'$ Band structure			
HeI[a] [2]	NeI[a] [2]	TPES[b]	Assignments
12.240	12.240	12.243 ± 0.009	**0,0**
-	-	12.267 ± 0.010	ν_9
12.300	12.305	12.303 ± 0.009	$\boldsymbol{\nu_7}$
-	-	12.331 ± 0.018	$\nu_7 + \nu_9$
12.368	12.370	12.365 ± 0.003	$\mathbf{2\nu_7}$
-	-	12.386 ± 0.003	$2\nu_7 + \nu_9$
-	-	12.420 ± 0.010	$2\nu_7 + 2\nu_9$
12.432	12.433	12.434 ± 0.006	$\mathbf{3\nu_7}$
-	-	12.464 ± 0.006	$3\nu_7 + \nu_9$
-	-	12.482 ± 0.006	$3\nu_7 + 2\nu_9$
12.496	12.496	12.498 ± 0.006	$\mathbf{4\nu_7}$
-	-	12.528 ± 0.011	$4\nu_7 + \nu\nu_9$
12.561	12.555	12.556 ± 0.005	$\mathbf{5\nu_7}$
-	-	12.572 ± 0.003	$5\nu_7 + \nu_9$
-	-	12.592 ± 0.009	$5\nu_7 + 2\nu_9$
12.629	12.620	12.614 ± 0.005	$\mathbf{6\nu_7}$
-	-	12.636 ± 0.003	$6\nu_7 + \nu_9$
-	12.681	12.673 ± 0.010	$\mathbf{7\nu_7}$

[a] Estimated uncertainties ± 0.010 eV [2].
[b] Largest deviation from the average of five independent measurements.

6. Conclusions

The threshold photoelectron spectrum of 1,1-C_2H_2FCl has been measured using synchrotron radiation. Eight photoelectron bands have been detected between the lowest adiabatic ionization energy at 10.034 ± 0.005 and 24 eV photon energy. The description and assignment of these bands were possible by using quantum chemical calculations. Besides singly ionized states doubly excited configurations were assigned. The first two bands show a rich and extensive vibrational structure. For each of these bands vibrational wavenumbers are measured and compared to the quantum chemical results. A very good correlation between the theoretical predictions and the experimental wavenumbers is obtained.

Acknowledgments

We are indebted to the University of Liège and the Freie Universitàt Berlin for financial support. RL and BL gratefully acknowledge the European Community for its support through its TMR (Contract EU-HPRI-1999CT-00028) and I3 (Contract R II 3 CT-2004-506008). DD's contribution was supported by the Belgian programme on Interuniversity Attraction Poles of the Belgian Science Policy (IAP no P6/19).

References

[1] Locht R, Dehareng D and Leyh B 2014 *Mol. Phys.* at press doi:10.1080/00268976.2013.842659

[2] Tornow G, Locht R, Kaufel R, Baumgärtel H and Jochims H-W 1990 *Chem. Phys.* **146** 115

[3] Locht R, Leyh B, Hottmann K and Baumgärtel H 1997 *Chem. Phys.* **220** 217

[4] Locht R, Leyh B, Hoxha A, Dehareng D, Jochims H-W and Baumgärtel H 2000 *Chem. Phys.* **257** 283

[5] Locht R, Leyh B, Denzer W, Hagenow G and Baumgärtel H 1991 *Chem. Phys.* **155** 407

[6] Carbonneau R, Bolduc E and Marmet P 1973 *Can. J. Phys.* **51505** Carbonneau R and Marmet P 1973 *Can. J. Phys.* **51** 2202 Carbonneau R and Marmet P 1974 *Phys. Rev.* A **9** 1898

[7] Marmet P 1979 *Rev. Sci. Instrum.* **50** 79 and references therein

[8] Locht R, Dehareng D and Leyh B 2012 *J. Phys. B: At. Mol. Opt. Phys.* **45** 115101

[9] Frisch M J *et al* 2009 *Gaussian 09, Revision A.02* (Wallingford, CT: Gaussian, Inc.)

[10] Dunning T H Jr 1989 *J. Chem. Phys.* **90** 1007

[11] Cizek J 1969 Adv. *Chem. Phys.* **14** 35

[12] Scuzeria G E and Schaefer H F III 1989 *J. Chem. Phys.* **90** 3700

[13] Zhao Y and Truhlar D G 2008 *Theor. Chem. Ace.* **120** 215

[14] Hegarty D and Robb M A 1979 *Mol. Phys.* **38** 1795

[15] Eade R H E and Robb M A 1981 *Chem. Phys. Lett.* **83** 362

[16] Bernardi F, Bottini A, McDougall J J W, Robb M A and Schlegel H B 1984 *Faraday Symp. Chem. Soc.* **19** 137

[17] Van Vaillie C and Amos R D 2000 *Chem. Phys. Lett.* **317** 159

[18] Irikura K K, Johnson R D III and Kacker R N 2005 *J. Phys. Chem.* A **109** 8430

[19] Tornow G 1981 *Diplomarbeit* Freie Universität Berlin, Berlin, Germany

[20] Kaufel R 1985 *PhD Dissertation* Freie Universität Berlin, Berlin, Germany

[21] Mohr P J and Taylor B N 1999 *J. Phys. Chem. Ref. Data* **28** 1713

[22] Mohr P J and Taylor B N 1713 *J. Phys. Chem. Ref. Data* **28** 1999 Mohr P J, Taylor B N and Newell D B 2008 *Rev. Mod. Phys.* **80** 633

[23] Locht R, Leyh B, Dehareng D, Hottmann K and Baumgârtel H 2010 *J. Phys. B: At. Mol. Opt.Phys.* **43** 015102 Locht R, Leyh B, Hottmann K and Baumgärtel H 1997 *Chem. Phys.* **220** 217 Hoxha A, Locht R, Leyh B, Dehareng D, Hottmann K, Jochims H-W and Baumgärtel H 2000 *Chem. Phys.* **256** 239

[24] Herzberg G 1967 *Molecular Spectra and Molecular Structure: I. Spectra of Diatomic Molecules* (Princeton, NJ: Van Nostrand) p 438 chapter 7